Conformational Origin of the Aggregation of Recombinant Human Factor VIII†

Adeola O. Grillo,[‡,#] Karen-Leigh T. Edwards,[‡,§] Ramesh S. Kashi,[||] Krista M. Shipley,[‡,⊥] Lina Hu,[||] Marc J. Besman,[||] and C. Russell Middaugh*[,‡]

Department of Pharmaceutical Chemistry, University of Kansas, Lawrence, Kansas 66046 and Hyland Immuno Division, Baxter Healthcare Corporation, Duarte, California 91010

Received July 5, 2000

ABSTRACT: Aggregation of proteins is a major problem in their use as drugs and is also involved in a variety of pathological diseases. In this study, biophysical techniques were employed to investigate aggregate formation in the pharmaceutically important protein, recombinant human factor VIII (rhFVIII). Recombinant human factor VIII incubated in solution at 37 °C formed soluble aggregates as detected by molecular sieve chromatography and dynamic light scattering. This resulted in a corresponding loss of biological activity. Fluorescence and CD spectra of the thermally stressed rhFVIII samples did not, however, suggest significant differences in protein conformation. To identify conformational changes in rhFVIII that may be involved in rhFVIII aggregation, temperature and solutes were used to perturb the native structure of rhFVIII. Far-UV CD and FTIR studies of rhFVIII as a function of temperature revealed conformational changes corresponding to an increase in intermolecular β-sheet content beginning at approximately 45 °C with significant aggregation observed above 60 °C. Fluorescence and DSC studies of rhFVIII also indicated conformational changes initiating between 45 and 50 °C. An increase in the exposure of hydrophobic surfaces was observed beginning at approximately 40 °C, as monitored by increased binding of the fluorescent probe, bis-anilinonaphthalene sulfonic acid (bis-ANS). Perturbation by various solutes produced several transitions prior to extensive unfolding of rhFVIII. In all cases, a common transition, characterized by an increase in the wavelength of the fluorescence emission maximum of rhFVIII from approximately 330 to 335 nm, was observed during thermal and solute perturbation of factor VIII. Moreover, this transition was correlated with an increased association of factor VIII upon incubation at 37 °C in the presence of various solutes. These results suggest that association of rhFVIII in solution was initiated by a small transition in the tertiary structure of the protein which produced a nucleating species that led to the formation of inactive soluble aggregates.

Factor VIII (FVIII),[1] a multidomain, high molecular weight (approximately 280 kDa) blood coagulation glycoprotein, is deficient in hemophilia A. In the blood coagulation cascade, FVIII acts as a cofactor of factor IXa for the activation of factor X on membranes (*1*). The active form of FVIII (FVIIIa), which binds to platelets in the factor X activation complex, is produced by the limited proteolysis of FVIII by thrombin (*2*−*6*).

Current treatment for hemophilia A includes the administration of recombinant human factor VIII (rhFVIII) produced in CHO cells (*7*). The protein is synthesized as a 2351-residue single-chain precursor from which a 19-residue signal peptide is cleaved upon translocation into the endoplasmic reticulum. Glycosylation of the protein takes place in the endoplasmic reticulum, and proteolytic processing to heavy and light chains occurs in the Golgi (*8*). The single-chain precursor is comprised of six domains in the order (NH_2)-A1-A2-B-A3-C1-C2(COOH). Domains A1, A2, and all or part of the B-domain make up the heavy chain, while domains A3, C1, and C2 comprise the light chain (*9*, *10*). The two polypeptide chains are associated by a metal ion between the A1 domain of the heavy chain and the A3 domain of the light chain (*3*, *10*−*13*). The triplicated A domains of factor VIII are 35−40% homologous to each other, the triplicated A domains in factor V, and to the copper-binding protein ceruloplasmin (*5*, *10*). Although calcium has been implicated in the metal-dependent association of the subunits (*14*, *15*), electron spin resonance and atomic absorption spectroscopy of factor VIII indicate the presence of copper (I) in a 1:1 mole ratio to factor VIII (*16*, *17*).

† Funding provided by Hyland Immuno Division, Baxter Healthcare Corporation, Duarte, CA, 91010.

* To whom correspondence should be addressed. Department of Pharmaceutical Chemistry, University of Kansas, 2095 Constant Avenue, Lawrence, KS 66047. Telephone: 785-864-5813. Fax: 785-864-5814. E-mail: middaugh@ukans.edu.

‡ Department of Pharmaceutical Chemistry, University of Kansas, Lawrence, KS.

§ Present address: Biogen Inc., Cambridge, MA.

|| Baxter Healthcare Corporation, Hyland Immuno Division, Duarte, CA.

⊥ Present Address: Graduate Group in Biophysics, University of California, San Francisco, CA.

Present address: Schering-Plough Research Institute, Kenilworth, NJ.

[1] Abbreviations: bis-ANS, bis-anilinonaphthalene sulfonic acid; CD, circular dichroism; CHO, Chinese Hamster Ovary cells; DSC, differential scanning calorimetry; EGTA, ethylene glycol tetraacetic acid; FVIIIa, activated factor VIII; FIXa, activated factor IX; FTIR, Fourier transform infrared spectroscopy; GdnHCl, guanidine hydrochloride; HP-SEC, high performance size-exclusion chromatography; MOPS, 3-(*N*-morpholino) propane sulfonic acid; rhFVIII, recombinant human factor VIII.

10.1021/bi001547t CCC: $20.00 © 2001 American Chemical Society
Published on Web 12/20/2000

Scanning transmission electron microscope studies of FVIII show that the three-dimensional structure of the molecule consists of a globular core made up of the A1−A2 domains of the heavy chain linked to the light chain and a peripheral satellite structure extending from the globular core made of the B domain of the heavy chain (*18*). A high-resolution crystal structure of the C2 domain has recently been reported (*19*), but details of the overall structure remain unknown. In addition to the metal ion linkage between the A1 and A3 domains, apolar interactions have also been implicated in the association (*20*).

Under certain conditions, it has been found that recombinant human factor VIII has a tendency to aggregate, a propensity potentially detrimental to its use as a drug substance. Aggregation of proteins appears to be most often associated with structural changes in the molecule (*21*). For example, structural changes in proteins that lead to exposure of apolar sites often result in protein aggregation and loss of biological activity. Although it was originally thought that protein aggregation was a consequence of extensive unfolding, it is becoming apparent that more subtle alterations in protein structure may often be responsible for associative behavior (*21*−*23*). To elucidate possible structural changes in rhFVIII that may be involved in protein aggregation and loss of biological activity, the factor VIII molecule has been characterized by a variety of techniques using temperature and solutes as structural perturbants. Evidence is presented for a unique structural transition in the molecule that may initiate the aggregation process.

MATERIALS AND METHODS

Time Course of Soluble Aggregate Formation of rhFVIII at 37 °C. rhFVIII bulk drug substance (approximately 0.5 mg/mL in buffer containing Tris, NaCl, $CaCl_2$, and Tween-80), obtained from Baxter Healthcare Corporation, was sterile-filtered and placed in a 37 °C incubator. Samples were withdrawn at various time intervals and stored frozen at −70 °C until examination.

Detection of Soluble Aggregates and Determination of Aggregate Size. High performance-size exclusion chromatography analysis was performed using two analytical TSK gel filtration columns, G6000 PWXL and G4000 PWXL (TosoHaas, Montgomeryville, PA), connected in series. Gel filtration was carried out under isocratic conditions (0.65 mL/min) in an aqueous buffer consisting of 50 mM Tris, 400 mM NaCl, 5 mM $CaCl_2$, and 0.05% NaN_3, pH 7.0. Elution of protein was monitored using a fluorescence detector, with excitation at 285 nm and emission at 335 nm. Dynamic light scattering measurements were performed at 25 °C with a Brookhaven BI-9000AT digital autocorrelator and a BI-200SM laser light scattering goniometer system equipped with a helium−neon-diode laser operating at 532 nm (Brookhaven Instruments Corporation, Holtsville, NY). A scattering angle of 90° was employed, and data was collected for 90 s. The autocorrelation function was analyzed by the methods of cumulants and a nonnegatively constrained least squares procedure (NNLS), and the hydrodynamic radius was calculated from the Stokes−Einstein equation. The rhFVIII samples were diluted to approximately 0.1 mg/mL prior to data collection.

Determination of rhFVIII Clotting Activity. rhFVIII clotting activity was determined by the one-stage activated partial thromboplastin time (APTT) assay using micronized silica as an activator and rhFVIII deficient plasma as a substrate. The APTT assay was performed using a COAG-A-MATE coagulation analyzer (Organon Teknika Corporation, Durham, NC). rhFVIII samples were added to FVIII-deficient plasma, and the clotting time was measured. The activities of the rhFVIII samples were then obtained from a calibration curve constructed using the clotting times determined from various dilutions of a lyophilized reference concentrate of known activity.

Effect of Aggregate Formation on rhFVIII Structure. Diluted rhFVIII samples (approximately 0.1 mg/mL) were used for all experiments. Circular dichroism spectra were obtained with a Jasco J-720 spectropolarimeter (Tokyo, Japan), calibrated with ammonium *d*-camphor-10-sulfonate. Measurements were performed at 25 °C in a 0.1-cm path length cell. The samples were scanned from 260 to 200 nm at a resolution of 0.1 nm and a scan speed of 20 nm/min. Buffer absorption prevents data from being obtained below 200 nm. Three accumulations of spectra were obtained for each sample and averaged. Fluorescence spectra were measured with a PTI QM-1 spectrofluorometer (Monmouth Junction, NJ). The samples were excited at 280 nm, and the emission was monitored from 300 to 450 nm. Excitation and emission slit widths were set at 4 and 3 nm, respectively. The emission spectra of the samples were acquired at 25 °C, and three scans were averaged with subtraction of spectra of buffer solutions. The fluorescence emission spectra of the gel-filtration fractionated native and aggregate species of a sample incubated at 37 °C for 9 days were also obtained.

Effect of Thermal Stress on rhFVIII. All thermal experiments were conducted in 10 mM MOPS buffer, pH 7, containing 4 mM $CaCl_2$ and 150 mM NaCl. The heat capacity of rhFVIII as a function of temperature was measured with a Calorimetry Sciences Corporation model 5100 nano-differential scanning calorimeter (Provo, Utah). The DSC thermogram was obtained from 2 to 100 °C at a scan rate of 1 °C/min. A protein concentration of 3.58 mg/mL was employed. A thermogram of the buffer was also obtained and subtracted from that of the protein solution. The effect of temperature on rhFVIII tertiary structure was analyzed by obtaining intrinsic fluorescence emission spectra of rhFVIII, and of the hydrophobic probe, bis-anilinonaphthalene sulfonate, in the presence of rhFVIII from 10 to 85 °C. A protein concentration of 0.1 mg/mL was again used. The temperature was varied through a peltier device integrated into the fluorometer sample compartment under the control of the fluorescence acquisition software. Emission scans were obtained at 5 °C intervals with incubation at each temperature for 3 min prior to data acquisition, a time sufficient for spectral changes to be complete. Intrinsic fluorescence emission spectra were obtained by excitation at 280 nm with emission monitored from 295 to 450 nm. The excitation and emission slit widths were set at 2 nm. The buffer was scanned at 25 °C and subtracted from each spectrum. The wavelength of the fluorescence emission maximum as a function of temperature was determined from first derivative spectra, which permits wavelength maximum to be measured with a precision of approximately 0.1 nm. rhFVIII samples (0.1 mg/mL) in the presence of 4 μM bis-ANS were excited at 385 nm and emission was monitored from 400 to 600 nm. The excitation and emission slit widths

were set at 2 and 4 nm, respectively. The weak emission spectrum of 4 μM bis-ANS in buffer at 25 °C was used as blank. The effect of temperature on rhFVIII secondary structure was monitored by CD and FTIR. Temperature was varied at a rate of 0.25 or 1 °C/min with the CD signal monitored at 215 nm. In addition, complete spectra were obtained at a scan rate of 10 nm/min at 5 °C intervals from 10 to 90 °C. FTIR spectra were obtained with a Magna-IR 560 spectrometer (Nicolet Madison, WI). Lyophilized protein (approximately 4.5 mg) was dissolved in 1 mL of D_2O (final buffer composition, 30 mM MOPS, 6 mM $CaCl_2$, pD 7). Measurements were obtained in an attenuated total reflectance mode, using a 45° ZnSe, 12-reflection multi-bounce cell. A 256-scan interferogram was collected in single beam mode with a resolution of 4 cm^{-1} for each spectrum. Spectra were collected at 27 °C and 30 to 90 °C at 5 °C intervals with incubation for 3 min prior to each data acquisition. Buffer spectra were also obtained at each temperature and subtracted from the protein spectra using a straight baseline between 1770 and 2050 cm^{-1} as the criterion for correct subtraction. The resulting blank-subtracted spectra were then smoothed with a 5-point Savitsky−Golay function. Second-derivative analysis was used to identify band components in the amide-I′ region. Curve-fitting was performed with the program PeakSolve (Galactic Industries Corporation) using a mixed Gaussian−Lorentzian function. Turbidity measurements of 0.1 mg/mL rhFVIII solutions were obtained with a HP 8453 UV−Visible spectrophotometer (Waldbronn Germany). The optical density at 350 nm was monitored from 10 to 90 °C at 1 or 0.5 °C intervals with 1 min incubation at each temperature.

Effect of Chemical Stress on rhFVIII. rhFVIII (0.1 mg/mL) was incubated with increasing concentrations of solute at room temperature for either 30 min (propanol and EGTA) or overnight ($LiClO_4$ and GdnHCl). Samples were excited at 280 nm, and the fluorescence emission spectra were monitored from 295 to 450 nm, employing excitation and emission slit widths of 2 nm. The effect of propanol and GdnHCl concentrations on the mean diameter of rhFVIII was also examined employing dynamic light scattering measurements as a function of incubation time at 37 °C as described above. Protein concentration in the incubated samples was 0.1 mg/mL. The samples were incubated at room temperature for one (propanol) or 3 h (GdnHCl) and filtered prior to data collection. The results were corrected for viscosity employing literature values of the temperature-dependent viscosity of propanol and GdnHCl (*24*, *25*).

RESULTS

Effect of Incubation at 37 °C on rhFVIII Aggregation and Structure. rhFVIII samples were incubated at 37 °C for up to 7 days and frozen until examination. The effect of incubation time on the formation of higher molecular weight species was analyzed by high performance size exclusion chromatography and dynamic light scattering. Size exclusion chromatography analysis of the rhFVIII samples showed an increase in population of soluble rhFVIII aggregates with time (Figure 1, panel A), with the population of higher molecular weight material increasing from zero to approximately 26% at the end of 7 days. Data analyses of dynamic light scattering measurements by NNLS showed that the samples were heterogeneous, usually containing two

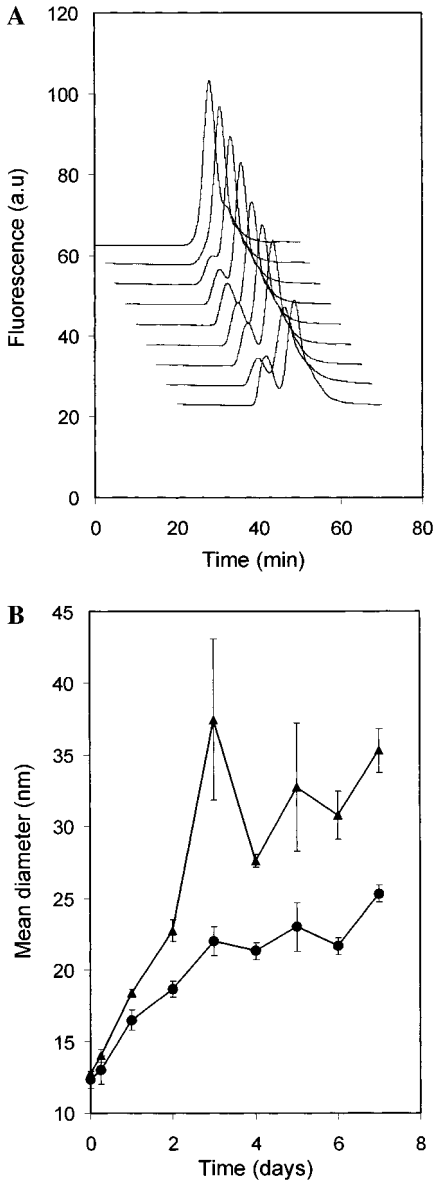

FIGURE 1: (A) HP-SEC analysis of rhFVIII samples showing formation of aggregates with time. The data for the incubation time points have been stacked for easy visualization. From top to bottom: 0 h, 6 h, 1 day, 2 day, 3 day, 4 day, 5 day, 6 day, and 7 day incubation time points. Gel filtration performed in 50 mM Tris, 400 mM NaCl, 5mM $CaCl_2$, 0.05% NaN_3, pH 7.0. The flow rate was 0.65 mL/min. (B) Dynamic light scattering analysis of rhFVIII samples as a function of incubation time. The mean diameters obtained by second-order cumulant (triangles) and NNLS (circles) analysis are shown. Protein concentration was ~0.1 mg/mL.

populations and in a few occasions, three. The size of the major population (greater than 99% by number and weight) in the samples ranged between 9 and 14 nm, while the size of the minor populations ranged between 25 and 55 nm. An increase in the mean size of rhFVIII in the samples was observed with time from approximately 12 nm to between 25 and 35 nm after 7 days (Figure 1, panel B). A loss in biological activity of up to 15% was also observed over this time period, as determined by a one-stage activated partial thromboplastin time assay (Table 1). Control experiments performed to examine the effect of freezing and thawing on factor VIII showed that up to three freeze−thaw cycles do not cause aggregation or result in loss of biological activity (data not shown).

Table 1: Biological Activity and Extent of Aggregation of RhFVIII Samples as a Function of Incubation Time at 37 °C[a]

time	% activity	% aggregation
0 h	100	0
6 h	101	0
1 day	96	10
2 days	97	15
3 days	90	20
4 days	92	20
5 days	89	20
6 days	92	18
7 days	85	26

[a] Activity was determined from a one-stage activated partial thromboplastin time assay and the percentage of aggregation from the data shown in Figure 1.

Fluorescence and CD spectra of rhFVIII, after various periods of incubation up to 7 days at 37 °C, were also determined. The native CD spectrum of rhFVIII manifested a minimum at 217 nm, indicative of a protein with a high β-structure content (Figure 2, panel A) (*26*). No significant differences in CD spectra were detected among the variably aggregated rhFVIII samples (not illustrated). Similar results were obtained with intrinsic fluorescence measurements. The fluorescence emission spectra of fractionated native and aggregated factor VIII are shown in Figure 2, panel B. The fluorescence emission maximum of native rhFVIII occurs at approximately 330 nm, suggesting that the tryptophan residues in the rhFVIII molecule are on the average relatively buried. The fluorescence emission spectra of the thermally perturbed rhFVIII samples were also comparable within experimental error (not shown). Although the fluorescence intensity of the purified aggregate species was quenched as compared to that of the native protein, there were no detectable differences in the wavelength of the emission maxima of the two species (Figure 2, panel B).

Effect of Temperature on rhFVIII Structure. To investigate possible changes in rhFVIII structure that may be involved in the observed protein association, rhFVIII was subjected to thermal stress. Differential scanning calorimetry, as well as fluorescence, CD, and FTIR spectroscopies were used to monitor the effect of temperature on rhFVIII structure. A DSC thermogram of rhFVIII (Figure 3) reveals several small but reproducible transitions within the temperature range studied in addition to a major transition centered near 58 °C. The magnitude of this major transition was, in fact, very small, requiring very high concentrations of protein (approximately 3.5 mg/mL) to be observed (unfolding transitions can normally be seen with this instrument at 1/10 the concentration of factor VIII employed). Unfortunately, the determination of an associated enthalpy change was not possible, since this transition was irreversible. Therefore, spectroscopic methods were employed to further explore the nature of these transitions.

The effect of temperature on rhFVIII tertiary structure was examined by monitoring the change in rhFVIII intrinsic fluorescence intensity and the position of the emission maximum as a function of temperature. The emission maximum of rhFVIII at 25 °C occurs at approximately 330 nm. This wavelength was therefore used to monitor the change in fluorescence intensity as temperature was increased (Figure 4, panel A). The fluorescence intensity of rhFVIII at 330 nm displayed the expected linear decrease with

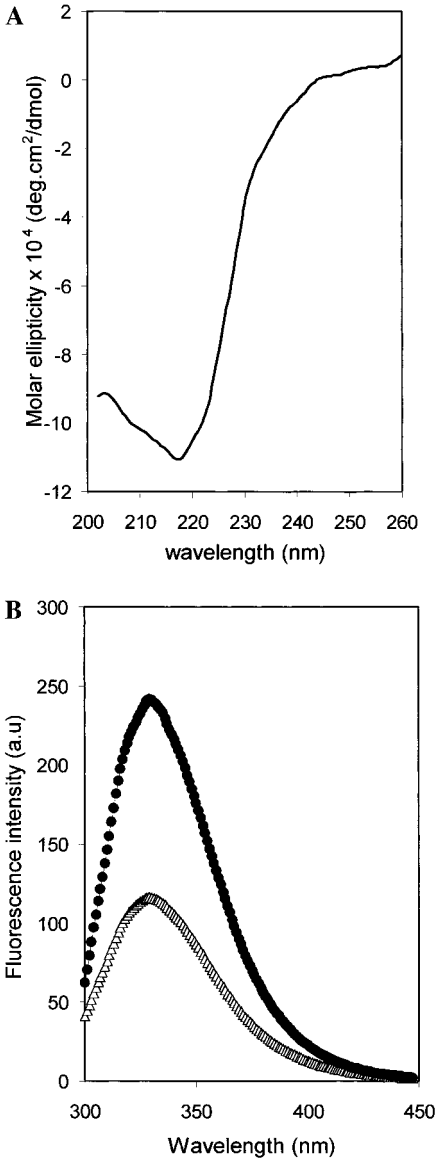

FIGURE 2: (A) Far-UV CD spectrum of rhFVIII at 25 °C. The spectrum shown is an average of three accumulations. (B) Fluorescence emission spectra of fractionated native (13.25 μg/mL, circles) and aggregate (19.17 μg/mL, triangles) species in 25 mM Tris, 300 mM NaCl, 4 mM $CaCl_2$, pH 7. The samples were excited at 280 nm.

temperature (*27*) with a transition observed between 45 and 65 °C. The position of the emission maximum of rhFVIII spectra also changes as a function of temperature with a transition observed between 50 and 75 °C (Figure 4, panel B). A relatively small increase of 5 nm in emission maximum position was observed over the temperature range studied. This increase in emission maximum position presumably reflects some increase in exposure of one or more buried tryptophan residues at higher temperatures. The protein is not, however, extensively unfolded over the temperature range monitored since the emission maximum position does not shift to 350−355 nm, the wavelength typically observed for indole in aqueous environments. The transition observed in the wavelength of the emission maximum seems to occur at temperatures similar to that of the major transition observed in the DSC experiments, but appears after the deviation from linearity observed in the fluorescence intensity measurements.

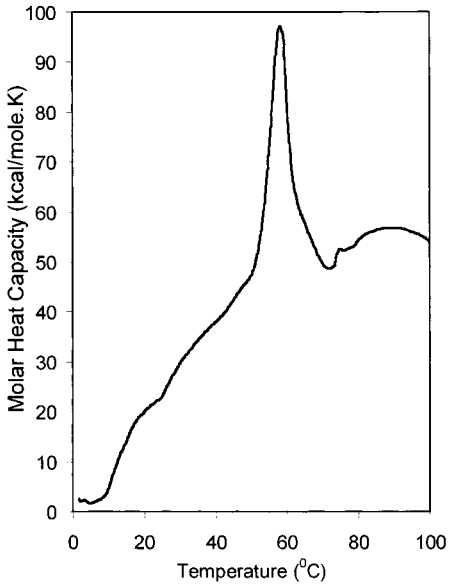

FIGURE 3: DSC thermogram of rhFVIII from 2 to 100 °C. Protein concentration was 3.58 mg/mL in 10 mM MOPS, 150 mM NaCl, 4 mM $CaCl_2 \cdot H_2O$, pH 7. The sample was scanned at 1 °C/min.

To further explore the effect of temperature on rhFVIII structure, the binding of the fluorescent dye bis-ANS to rhFVIII was monitored as a function of temperature. Bis-ANS is essentially nonfluorescent in aqueous solutions but becomes appreciably fluorescent in nonpolar environments (*28*). In addition, the fluorescence emission maximum of the dye shifts to lower wavelengths in nonpolar milieu. Thus, the dye is a useful probe of the degree of exposure of hydrophobic sites as the structure of a protein is perturbed (*29*, *30*). In addition, the anionic nature of the dye has been shown to contribute to its interaction with cationic sites on proteins (*31*). The binding of bis-ANS to factor VIII and to factor VIII subunits has been previously reported, with two hydrophobic sites observed on the surface of factor VIII, in addition to intersubunit hydrophobic sites between the heavy and light chains (*20*). The fluorescence intensity of bis-ANS in buffer is negligible as compared to the intensity of the dye in the presence of rhFVIII (data not shown). The effect of temperature on the intensity of 4 μM bis-ANS in the presence of 0.1 mg/mL rhFVIII is shown in Figure 5. Intensity changes were monitored at 500 nm. An increase in the binding of bis-ANS to rhFVIII is indicated by an increase in bis-ANS intensity between 40 and 60 °C after which the fluorescence declines (Figure 4, panel A). The spectral changes again coincide with the transitions detected by intrinsic fluorescence emission and DSC. Thus, the temperature-induced transitions observed employing bis-ANS binding, DSC, and intrinsic fluorescence appear to reflect a common conformational change in the protein that results in an increased exposure of apolar residues to the solvent.

The effect of temperature on rhFVIII secondary structure was investigated by obtaining far-UV CD and FTIR spectra as a function of temperature. Increasing temperature resulted in an increase in β-sheet content as suggested by increases in the negative CD ellipticity at 215 nm (Figure 6) with the transition beginning at approximately 45 °C and the midpoint occurring near 60 °C. The CD results were supported by FTIR data. The effect of temperature on the FTIR spectrum of rhFVIII in the amide I′ region is shown in Figure 7, panel

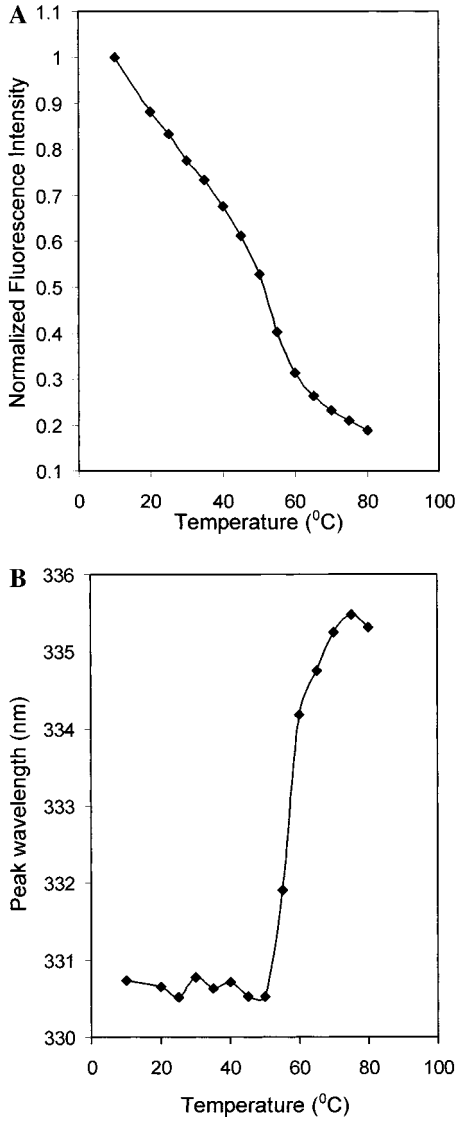

FIGURE 4: (A) Effect of temperature on rhFVIII fluorescence emission intensity at 330 nm. The sample was equilibrated at each temperature for 3 min prior spectra acquisition. The intensity values were normalized by dividing the intensities at 330 nm for each measured temperature by the intensity at 330 nm for the measurement taken at 10 °C. Protein concentration was 0.1 mg/mL in 10 mM MOPS, 4 mM $CaCl_2$, 150 mM NaCl, pH 7. (B) Effect of temperature on the fluorescence emission maximum of rhFVIII.

A, while deconvoluted peaks for spectra obtained at 27 and 90 °C are displayed in Figure 7, panels B and C, respectively. Deconvolution of the amide I′ region of rhFVIII spectra revealed 10 individual peaks at 1608, 1618, 1627, 1637, 1646, 1654, 1661, 1667, 1675, and 1684 cm^{-1}. The peak at 1608 cm^{-1} is probably due to absorbance by side chains (*32*). The peak at 1654 cm^{-1} has been assigned to α-helices, the peaks at 1661, 1667, and 1675 cm^{-1} have been assigned to turns, and the peak at 1646 cm^{-1} has been assigned to unordered structures (*32*). The peak at 1637 cm^{-1} was assigned to β-sheets, while the peaks at 1618, 1627, and 1684 cm^{-1} have been assigned to intermolecular β-sheet (*33*−*37*). A characteristic signature of intermolecular β-sheet formation is the presence of a low-frequency band at approximately 1620 cm^{-1} and a weaker high-frequency band at approximately 1682 cm^{-1} (*37*). An increase in temperature results in an increase in absorbance at 1618 and 1684 cm^{-1}, indicating an increase in intermolecular β-sheets (Figure 7,

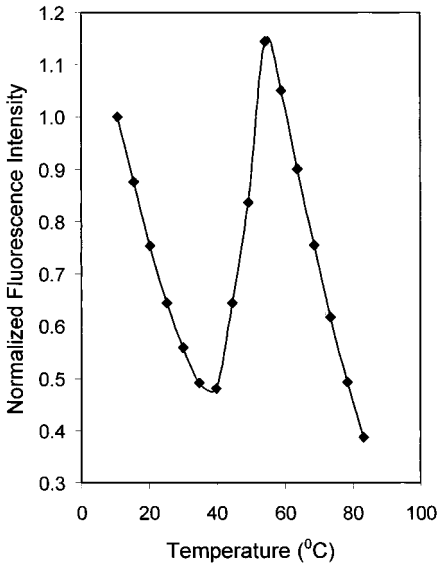

FIGURE 5: Effect of temperature on the fluorescence of bis-ANS in the presence of rhFVIII (bis-ANS emission intensity measured at 500 nm). A protein concentration of 0.1 mg/mL and bis-ANS concentration of 4 μM was used in 10 mM MOPS, 150 mM NaCl, 4mM $CaCl_2$, pH 7. Samples were incubated at each temperature for 3 min prior to spectra acquisition.

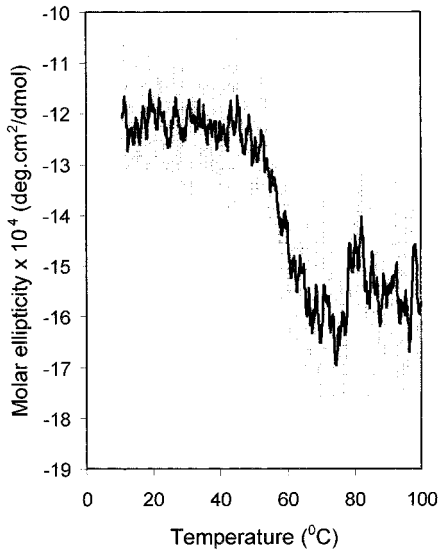

FIGURE 6: Effect of temperature on the molar ellipticity of rhFVIII at 215 nm. A moving average of the raw data is shown by the dark line for easier visualization of the temperature profile.

panels B and C). A plot of the absorbance at 1618 cm^{-1} as a function of temperature shows that the absorbance of rhFVIII at 1618 cm^{-1} starts to increase at approximately 45 °C, implying the initiation of intermolecular β-sheet formation at that temperature (Figure 7, panel D). Turbidity measurements of rhFVIII monitored at 350 nm (OD_{350}) showed an increase beginning at approximately 75 °C (data not shown). The increase in turbidity observed could account for the slight decrease in CD signal observed at approximately 75 °C (Figure 6). All of the thermal transitions detected by DSC, fluorescence, CD, and FTIR were found to be irreversible (data not shown) as examined by the return of samples to pretransition temperatures.

Effect of Solutes on rhFVIII Structure. To further probe structural changes in rhFVIII, compounds that typically perturb protein structure were utilized. The solutes selected were GdnHCl, urea, $LiClO_4$, and propanol (*38*). These agents were observed to perturb the structure of rhFVIII to various extents. A common effect produced by all of the compounds at lower concentrations was a transition in rhFVIII structure characterized by a shift in the wavelength of the fluorescence emission maximum of rhFVIII from 330 nm to 334−336 nm (Figure 8). More extensive unfolding is seen in 5 M GdnHCl, as evidenced by the shift of the fluorescence wavelength emission maximum to 350 nm. Complete structural disruption was not obtained with the other agents at the highest concentrations utilized. At least three transitions are observed in the disruption of rhFVIII induced with GdnHCl, two transitions with urea, and one with propanol and $LiClO_4$. Most interestingly, however, the first transition observed in each case is characterized by a shift in the emission maximum from 330 to 334−336 nm, implying a related structural alteration. The transition observed by the thermal perturbation of rhFVIII is also characterized by a shift in the intrinsic emission maximum of rhFVIII from 330 to 335 nm (Figure 4, panel B). The simplest interpretation of these results is that the factor VIII molecule contains an inherently labile structural feature. To further examine this possibility, thermal and solute perturbants were combined. The effect of temperature on the wavelength of the emission maximum of rhFVIII in the absence and presence of GdnHCl (0.5 and 2 M) is shown in Figure 9, panel A. The presence of 0.5 M GdnHCl destabilizes the transition observed during the thermal perturbation of rhFVIII with the transition beginning approximately 15 °C lower than in the absence of GdnHCl. Again, however, in the presence of 0.5 M GdnHCl, a 5-nm shift in the wavelength of the emission maximum is observed (from 331 to 336 nm). The effect of 0.5 M GdnHCl on the response of rhFVIII to thermal stress as monitored by CD also shows a destabilization of approximately 10 °C in the midpoint of the transition (data not shown). In the presence of 2 M GdnHCl, which induces the 336-nm state, further perturbation by heat does not cause any further detectable alteration of the protein. Thus, this new form of the protein can only be further disrupted by higher concentrations of strong chaotropes such as GdnHCl and urea.

The effect of propanol and guanidine hydrochloride concentration on the propensity of rhFVIII to aggregate in solution, when incubated at 37 °C, was investigated by obtaining dynamic light scattering measurements of the stressed samples. In the presence of increasing concentrations of propanol, after an incubation time of 1 h at room temperature, the mean diameter of rhFVIII increased from about 20 to approximately 98 nm (Figure 9, panel B). Incubation of the samples at 37 °C resulted in further increases in the mean diameter of rhFVIII as a function of incubation time, with a maximum diameter of approximately 125 nm attained in 4 M propanol after 3 days (Figure 9, panel B). Further incubation did not show significant increases in size. Polydispersity indices for all factor VIII samples incubated at 37 °C in propanol were less than 0.2. It appears that these samples were relatively monodisperse and the size of the factor VIII particles in propanol increased uniformly with increased incubation time at 37 °C. In the presence of increasing GdnHCl concentrations after 3 h at room temperature, no significant differences in the mean diameter of rhFVIII were observed over the concentration

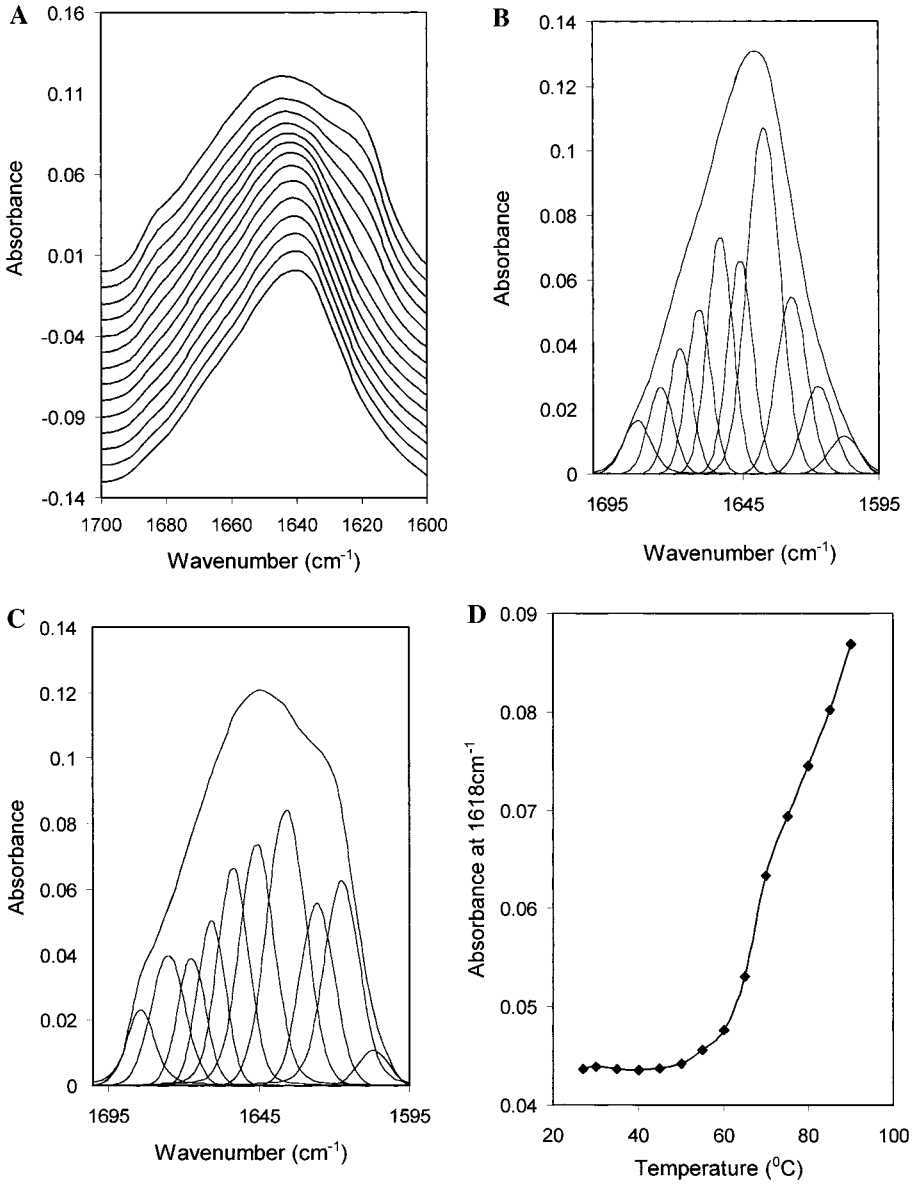

FIGURE 7: (A) Effect of temperature on the amide I′ IR spectrum of rhFVIII. The sample contained 4.5 mg of lyophilized rhFVIII in 30 mM MOPS, 6 mM $CaCl_2.H_2O$, pD 7, dissolved in 1 mL of D_2O. From bottom to top: 27 °C, 30−90 °C at 5 °C intervals. (B) Deconvolution of the amide I′ spectrum of rhFVIII obtained at 27 °C. (C) Deconvolution of the amide I′ spectrum of rhFVIII at 90 °C. (D) Effect of temperature on the absorbance of rhFVIII at 1618 cm^{-1}.

range studied (Figure 9, panel C). After incubation at 37 °C for 1 day, however, the mean diameter of rhFVIII particles at GdnHCl concentrations up to 1.5 M varied significantly with a maximum size of about 36 nm attained in 0.5 M GdnHCl (Figure 9, panel C). At concentrations above 1.5 M, the mean diameters of rhFVIII particles returned to their monomeric values. Incubation at 37 °C for longer times resulted in further increases in the mean diameters of the rhFVIII in GdnHCl concentrations up to 1.5 M, with a maximum size of approximately 50 nm obtained in 0.5 M GdnHCl after 4 days of incubation time. Increased incubation time at 37 °C did not result in significant increases in the sizes of rhFVIII particles above 1.5 M GdnHCl (Figure 9, panel C). Factor VIII samples incubated at 37 °C in the presence of GdnHCl were polydisperse except for samples with 0.5, 0.75, and 1 M GdnHCl incubated for 3 days and above.

The heavy and light chains of rhFVIII are held together by a metal ion believed to be calcium or copper (*15*−*17*). Thus, the effect of the metal chelator EGTA on rhFVIII structure was examined using CD and fluorescence. The addition of EGTA produces a decrease in rhFVIII fluorescence emission intensity, with no concomitant shift in peak position. No significant changes in rhFVIII secondary structure are observed with the addition of EGTA as monitored by CD (data not shown). The effect of EGTA on the response of rhFVIII to thermal stress was also monitored by fluorescence. The effect of temperature on the wavelength of the emission maximum of rhFVIII in the presence and absence of 40 mM EGTA is shown in Figure 10. The transition (increase in the wavelength of the fluorescence emission maximum) observed in the absence of EGTA is lowered by about 10 °C in the presence of EGTA. This result suggests the possible involvement of heavy chain/light chain interactions in this structural change. The effect of temperature on the secondary structure of rhFVIII in the presence of EGTA could not be monitored by CD due to absorption by EGTA in the far-UV region.

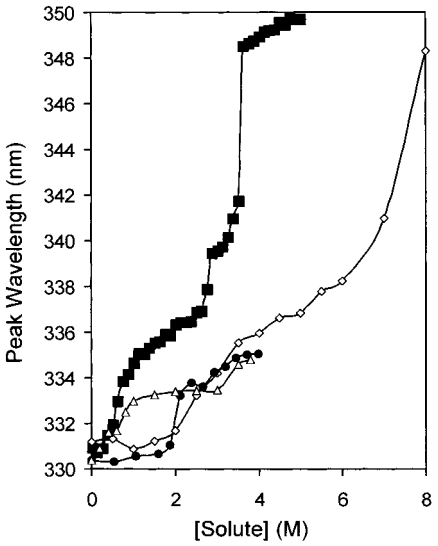

FIGURE 8: Effect of solute concentration on the wavelength of the fluorescence emission maximum of rhFVIII. GdnHCl is shown in squares, $LiClO_4$ is shown in triangles, urea is shown in diamonds, and propanol is shown in circles.

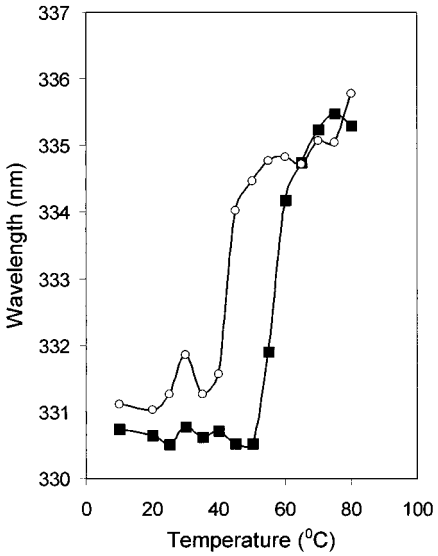

FIGURE 10: Effect of temperature on the fluorescence wavelength emission maximum of rhFVIII in the absence (squares) and presence (circles) of 40 mM EGTA.

DISCUSSION

The aggregation of proteins often appears to be produced by limited structural alterations of the native state rather than by complete unfolding of the protein. One candidate for these states are molten globule forms in which the secondary structure is essentially intact but the tertiary structure is substantially disrupted. Such states also appear somewhat expanded in size (a 10−20% increase in diameter) and more apolar as indicated by the binding of hydrophobic dyes such as ANS (*39*, *40*). In the case of the important pharmaceutical protein, rhFVIII, we find that incubation of rhFVIII at 37 °C results in the formation of soluble complexes. The slow kinetics of formation and the presence of an apparent lag period (no aggregate can be detected at 6 h) suggests some type of slow nucleation phenomenon may be involved in the aggregation process. The size and population of these aggregates increase with time, resulting in an increase in size from approximately 12 nm to between 25 and 35 nm, and a 26% aggregate population at the end of 7 days. The formation of these complexes also results in a partial loss of biological activity of approximately 15%. Spectroscopic measurements of thermally stressed unfractionated factor VIII did not, however, reveal species containing altered secondary and tertiary structure. This could simply reflect the low abundance of aggregated species in the samples examined. This seems unlikely to be the case, however, since isolation of the aggregated species itself does not find a form with an emission maximum of approximately 335 nm. This would seem to imply that if the 335 nm intermediate is involved in

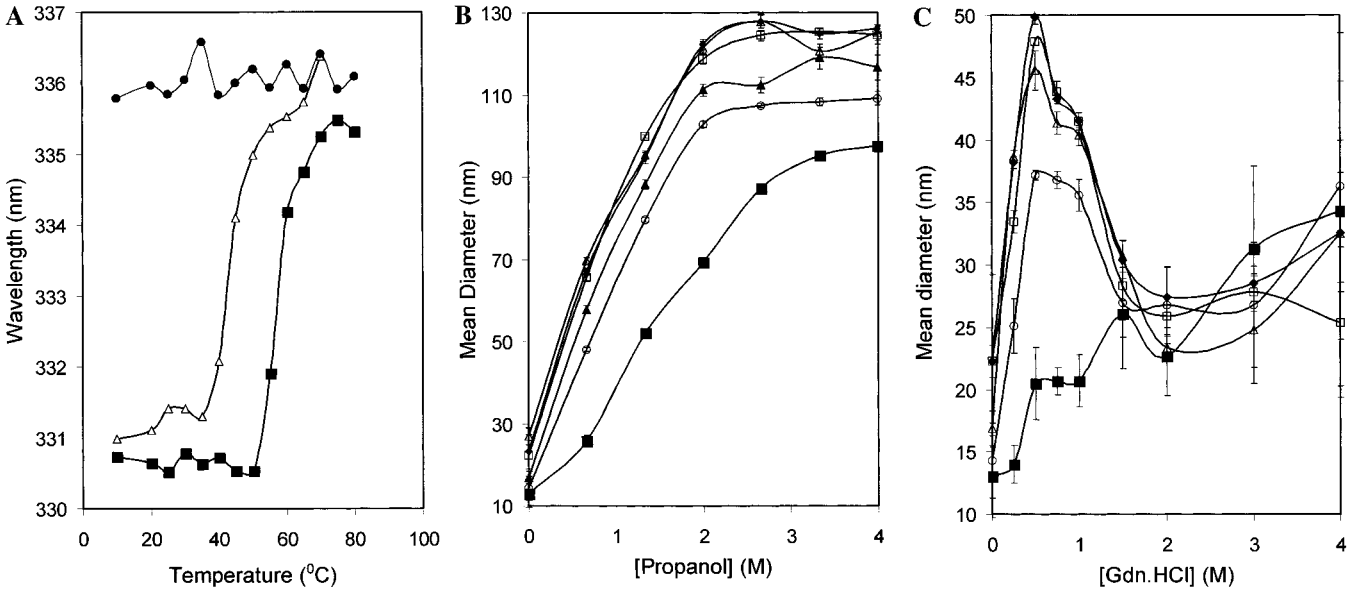

FIGURE 9: (A) Effect of guanidine hydrochloride concentration on the temperature dependence of the fluorescence emission maximum of rhFVIII: rhFVIII (squares), rhFVIII + 0.5 M GdnHCl (triangles), and rhFVIII + 2 M GdnHCl (circles). (B) Effect of propanol concentration and incubation time (at 37 °C) on rhFVIII size as determined by dynamic light scattering: time 0 (closed squares), day 1 (open circles), day 2 (closed triangles), day 3 (open squares), day 4 (closed diamonds), and day 5 (open triangles). (C) Effect of GdnHCl concentration and incubation time (at 37 °C) on rhFVIII size as determined by DLS: day 0 (closed squares), day 1 (open circles), day 2 (closed triangles), day 3 (open squares), day 4 (closed diamonds).

aggregation, it must be present in only limited amounts in the associated complexes themselves. Some quenching in the tryptophan fluorescence of the complexes is apparent, but the significance of this observation is unclear.

Characterization of the structural alteration of rhFVIII by temperature and solutes provides some insight into the nature of the 335-nm intermediate. Thermal perturbation profiles as monitored by DSC, intrinsic fluorescence, binding of bis-ANS, CD, and FTIR show a transition beginning near 45 °C (Figures 3−7). Formation of factor VIII aggregates at 47 °C is much more rapid than the results shown in Figures 1 and 2, but it is reasonable to assume that a temperature of 37 °C is sufficient to generate a small population of altered species that could initiate protein association. This is clear from the bis-ANS binding results where an increase in bis-ANS binding is evident below 40 °C indicating the presence of an altered factor VIII species. Fluorescence intensity changes are also consistent with this idea. This transition seems to involve some limited increase in exposure of apolar side chains (as judged by intrinsic fluorescence and the binding of bis-ANS). The transition also coincides with an increase in β-sheet content (as monitored by CD), which presumably corresponds to intermolecular β-sheet formation (as suggested by FTIR) as complexes associate. Formation of intermolecular β-sheets with increasing temperature has been observed for a large number of other proteins (*37*). In addition to the appearance of intermolecular β-sheet, a gradual disappearance of ordered secondary structure and the appearance of disordered polypeptide are also often observed with increasing temperature (*35*, *37*, *41*). In the case of rhFVIII, however, the formation of intermolecular β-sheet aggregates corresponds to only a slight decrease in native β-sheet structures and no detectable increase in disordered structures or a significant decrease in α-helical content.

To better understand the nature of the observed predenatural conformational transitions of rhFVIII, the effect of compounds that commonly disrupt protein structure on rhFVIII was examined. The intrinsic fluorescence spectral profile of rhFVIII as a function of various solute concentrations is characterized by an initial transition corresponding to an increase in the wavelength of the fluorescence emission maximum from approximately 330 to 335 nm. More extensive unfolding of the protein was achieved only at high concentrations of GdnHCl (approximately 4.5−5 M). We postulate that the initial transition observed with increasing solute concentration, is essentially the same structural change in each case since the wavelength shift is virtually identical within experimental errors. Thermal melts in the presence of 0.5 M GdnHCl and in the presence of the metal chelator EGTA show that the thermal transition is perturbed by these other agents. In the presence of 2 M GdnHCl, where the transition has presumably already been induced, increased temperature has no further effect on the peak position. Furthermore, the propensity for rhFVIII to aggregate in solution increases within the solute concentration range in which the 330 → 334−336 nm transition occurs. The size of rhFVIII increases in the presence of increasing concentrations of propanol (up to 4 M) with incubation at 37 °C resulting in further increases in size. Although significant differences in size are not initially observed in the presence of GdnHCl, incubation at 37 °C for 24 h results in aggregation of rhFVIII in GdnHCl concentrations up to 1.5 M. Aggregation is not observed, however, in rhFVIII in the presence of 1.5−4 M GdnHCl. The denaturing action of GdnHCl is thought to be due to the binding of the solute to proteins, resulting in the destruction of noncovalent interactions and thus, protein solubilization (*42*). Therefore, it seems most probable that the differences in the maximum mean diameter of rhFVIII observed in GdnHCl (50 nm) and propanol (125 nm) arise from the solubilizing effect of GdnHCl. In addition, although the 330 → 334−336 nm transition occurs between 0 and 1.5−2 M GdnHCl, maximum aggregation is observed at 0.5 M GdnHCl. The solubilizing effect of GdnHCl could also account for the decrease in aggregation observed above 0.5 M GdnHCl. Finally, the differences between the polydispersity of the samples incubated in propanol and the samples incubated in GdnHCl can be explained by the dual effects of the formation of a species at intermediate GdnHCl concentrations that induces aggregation and the solubilizing action of GdnHCl at higher solute levels. Aggregation of proteins in intermediate concentrations (0.5−1.5 M) of GdnHCl has previously been reported (*43*−*49*). The formation of aggregates at subdenaturation concentrations of GdnHCl is usually associated with partial unfolding of proteins, resulting in exposed apolar surfaces, and in a number of cases, increases in β-sheet content (*43*, *44*, *46*, *48*, *49*). The dissociation of oligomeric proteins, resulting in the exposure of previously buried hydrophobic surfaces, at low GdnHCl concentrations has also been implicated in aggregation (*45*, *46*). In total, these results provide strong evidence for the involvement of a species formed during the 330 → 334−336 nm transition in the aggregation of rhFVIII.

The destabilization of the thermal transition observed in the presence of a metal chelator suggests that this transition might involve an alteration in the interaction between the heavy and light chains of rhFVIII. Intersubunit apolar interactions have previously been shown through bis-ANS binding studies to be important for the metal ion-dependent association between the A1 and A3 subunits of the heavy and light chains, respectively (*15*, *20*). The isolated heavy and light chains of factor VIII each contain two surface-exposed bis-ANS binding sites, two of which are buried upon association of the chains. The metal ion-dependent reconstitution of factor VIII from the isolated heavy and light chains is inhibited in the presence of bis-ANS. In addition, displacement of the dye is observed upon addition of calcium ions, copper (II) ions and isolated light chain to the heavy chain−dye complex, suggesting the importance of apolar residues in the association of the heavy and light chains (*15*, *20*). Thus, a change in the subunit interface could well result in the exposure of hydrophobic sites at the subunit interface. Whatever the precise nature of this structural alteration, it is in many ways not "molten-globule"-like (*39*, *40*, *50*, *51*). Although there is no significant change in secondary structure, the easily induced alteration in tertiary structure appears to be of limited extent. There is no evidence yet for the expansion in size of factor VIII, although this might not be detectable under the conditions examined. The increase in apolarity implied by the dye binding studies is also relatively small as compared to the large increases seen when conventional molten globule forms appear and could also involve electrostatic interactions (*31*). We therefore conclude

that in some cases, fairly minor structural alterations can result in marked aggregation behavior. This result is perhaps not too surprising given the subtle relationship between protein structure, stability, association behavior, and related manifestations in pathological conditions such as sickle cell and Alzheimer's diseases, cryoglobulinemia, and cataract formation (*52*).

REFERENCES

1. van Dieijen, G., Tans, G., Rosing, J., and Hemker, H. C. (1981) *J. Biol. Chem. 256*, 3433−42.
2. Fulcher, C. A., Roberts, J. R., and Zimmerman, T. S. (1983) *Blood 61*, 807−11.
3. Fay, P. J., Anderson, M. T., Chavin, S. I., and Marder, V. J. (1986) *Biochim. Biophys. Acta 871*, 268−78.
4. Eaton, D., Rodriguez, H., and Vehar, G. A. (1986) *Biochemistry 25*, 505−12.
5. Kane, W. H., and Davie, E. W. (1988) *Blood 71*, 539−55.
6. Mann, K. G., Jenny, R. J., and Krishnaswamy, S. (1988) *Annu. Rev. Biochem. 57*, 915−56.
7. Neutzling, O. (1993) *Beitr. Infusionsther. 31*, 38−43.
8. Kaufman, R. J., Wasley, L. C., and Dorner, A. J. (1988) *J. Biol. Chem. 263*, 6352−62.
9. Toole, J. J., Knopf, J. L., Wozney, J. M., Sultzman, L. A., Buecker, J. L., Pittman, D. D., Kaufman, R. J., Brown, E., Shoemaker, C., and Orr, E. C. (1984) *Nature 312*, 342−7.
10. Vehar, G. A., Keyt, B., Eaton, D., Rodriguez, H., O'Brien, D. P., Rotblat, F., Oppermann, H., Keck, R., Wood, W. I., and Harkins, R. N. (1984) *Nature 312*, 337−42.
11. Fass, D. N., Knutson, G. J., and Katzmann, J. A. (1982) *Blood 59*, 594−600.
12. Andersson, L. O., Forsman, N., Huang, K., Larsen, K., Lundin, A., Pavlu, B., Sandberg, H., Sewerin, K., and Smart, J. (1986) *Proc. Natl. Acad. Sci. U.S.A. 83*, 2979−83.
13. Fay, P. J., Haidaris, P. J., and Smudzin, T. M. (1991) *J. Biol. Chem. 266*, 8957−62.
14. Fay, P. J. (1988) *Arch. Biochem. Biophys. 262*, 525−31.
15. Sudhakar, K., and Fay, P. J. (1998) *Biochemistry 37*, 6874−82.
16. Bihoreau, N., Pin, S., de Kersabiec, A. M., Vidot, F., and Fontaine-Aupart, M. P. (1994) *Eur. J. Biochem. 222*, 41−8.
17. Tagliavacca, L., Moon, N., Dunham, W. R., and Kaufman, R. J. (1997) *J. Biol. Chem. 272*, 27428−34.
18. Mosesson, M. W., Fass, D. N., Lollar, P., DiOrio, J. P., Parker, C. G., Knutson, G. J., Hainfeld, J. F., and Wall, J. S. (1990) *J. Clin. Invest. 85*, 1983−90.
19. Pratt, K. P., Shen, B. W., Takeshima, K., Davie, E. W., Fujikawa, K., and Stoddard, B. L. (1999) *Nature 1999 402*, 439−42.
20. Sudhakar, K., and Fay, P. J. (1996) *J. Biol. Chem. 271*, 23015−21.
21. Fields, G., Alonso, D., Stiger, D., and Dill, K. (1992) *J. Phys. Chem. 96*, 3974−81.
22. Carpenter, J. F., Kendrick, B. S., Chang, B. S., Manning, M. C., and Randolph, T. W. (1999) *Methods Enzymol. 309*, 236−55.
23. Speed, M. A., Wang, D. I., and King, J. (1996) *Nat. Biotechnol. 14*, 1283−7.
24. Mikhail, S. Z., and Kimel, W. R. (1963) *J. Chem. Eng. Data 8*, 323−328.
25. Kawahara, K., and Tanford, C. (1966) *J. Biol. Chem. 241*, 3228−32.
26. Johnson, W. C. J. (1988) *Annu. Rev. Biophys. Biophys. Chem. 17*, 145−166.
27. Guilbault, G. G. (1973) *Practical Fluorescence: Theory, Methods, and Techniques*, M. Decker, New York.
28. Rosen, C. G., and Weber, G. (1969) *Biochemistry 8*, 3915−20.
29. Stryer, L. (1965) *J. Mol. Biol. 1965 13*, 482−95.
30. Turner, D. C., and Brand, L. (1968) *Biochemistry* (1968) *7*, 3381−90.
31. Matulis, D., and Lovrien, R. (1998) *Biophys. J. 74*, 422−9.
32. Venyaminov, S. Y., and Kalnin, N. N. (1990) *Biopolymers 30*, 1243−57.
33. Byler, D. M., and Susi, H. (1986) *Biopolymers 25*, 469−87.
34. Prestrelski, S. J., Byler, D. M., and Liebman, M. N. (1992) *Proteins 14*, 440−5.
35. Clark, A. H., Saunderson, D. H., and Suggett, A. (1981) *Int. J. Pept. Protein Res. 17*, 353−64.
36. Ismail, A. A., Mantsch, H. H., and Wong, P. T. (1992) *Biochim. Biophys. Acta 1121*, 183−8.
37. Dong, A., Prestrelski, S. J., Allison, S. D., and Carpenter, J. F. (1995) *J. Pharm. Sci. 84*, 415−24.
38. Sadler, A. J., Micanovic, R., Katzenstein, G. E., Lewis, R. V., and Middaugh, C. R. (1984) *J. Chromatogr. 317*, 93−101.
39. Fink, A. L. (1995) *Annu. Rev. Biophys. Biomol. Struct. 24*, 495−522.
40. Dobson, C. M. (1994) *Curr. Biol. 4*, 636−40.
41. van Stokkum, I. H., Linsdell, H., Hadden, J. M., Haris, P. I., Chapman, D., and Bloemendal, M. (1995) *Biochemistry 34*, 10508−18.
42. Tanford, C. (1968) *Adv. Protein Chem. 23*, 121−282.
43. Kendrick, B. S., Carpenter, J. F., Cleland, J. L., and Randolph, T. W. (1998) *Proc. Natl. Acad. Sci. U.S.A. 95*, 14142−6.
44. Kendrick, B. S., Cleland, J. L., Lam, X., Nguyen, T., Randolph, T. W., Manning, M. C., and Carpenter, J. F. (1998) *J. Pharm. Sci. 87*, 1069−76.
45. Liang, S. J., Lin, Y. Z., Zhou, J. M., Tsou, C. L., Wu, P. Q., and Zhou, Z. K. (1990) *Biochim. Biophys. Acta 1038*, 240−6.
46. Nozais, M., Bechet, J. J., and Houadjeto, M. (1992) *Biochemistry 31*, 1210−5.
47. Mizobata, T., and Kawata, Y. (1995) *J. Biochem. (Tokyo) 117*, 384−91.
48. Swietnicki, W., Morillas, M., Chen, S. G., Gambetti, P., and Surewicz, W. K. (2000) *Biochemistry 39*, 424−31.
49. Webb, T., Jackson, P. J., and Morris, G. E. (1997) *Biochem, J. 321*, 83−8.
50. Arai, M., and Kuwajima, K. (2000) *Adv. Protein Chem. 53*, 209−82.
51. Fink, A. L. (1995) *Methods Mol. Biol. 40*, 343−60.
52. Middaugh, C. R., and Volkin, D. B. (1992) *Pharm. Biotechnol. 2*, 109−34.

BI001547T